J. Fluid Mech. (1975), *vol.* 70, *part* 2, *pp.* 321–332
Printed in Great Britain

Withdrawal of a stratified fluid from a vertical two-dimensional duct

By JORG IMBERGER
Departments of Mathematics and Mechanical Engineering,
University of Western Australia, Nedlands

AND CHRIS FANDRY
Department of Mathematics, Monash University,
Clayton, Victoria 3168, Australia

(Received 23 September 1974)

On the basis of a small Froude number theory it is shown that previous horizontal-duct models of the withdrawal of fluid from a stratified tank with a free surface and a fixed bottom are inappropriate at large times and that the flow should be modelled by that from an infinite vertical duct. The falling horizontal free surface in the tank is replaced by a vertically moving column of stratified fluid and the tank bottom is modelled by a stagnant pool of fluid below. This model is analysed and a solution uniformly valid in time is presented. The properties of the solution are then compared with existing theories and experiments.

1. Introduction

For much of the year the impounded waters of a storage reservoir are temperature-stratified. This stratification is most pronounced at the thermocline, but there is also usually a weak, nearly linear, temperature gradient throughout the hypolimnion where the intake structures of a reservoir are located. Without stratification the streamlines close to the intake would be essentially radial, but a vertical density gradient may produce buoyancy forces comparable to inertia forces, so that the water withdrawn comes from a thin horizontal layer at the level of the intake. This phenomenon is often called selective withdrawal.

Such layers have received a good deal of attention. Yih (1965) and later Kao (1965, 1970) established the dynamics of the layer when the fluid is inviscid. Koh (1966) investigated sink flow in a linearly stratified diffusive fluid of infinite extent. He neglected the inertia forces and made the usual boundary-layer-type simplifications. The flow was found to be self-similar and the solution exhibited a horizontally layered flow towards the sink. This solution conserved volume flux through a vertical section but, as shown by Imberger (1972), did not conserve momentum. The relation between Kao's (1970) and Koh's (1966) work was explained by Imberger (1972), who considered the withdrawal of fluid contained in an infinitely long, horizontal duct. He demonstrated that, provided that the Froude number F was small and the Rayleigh number Ra and the Reynolds number Re were large, the flow could be partitioned into three distinct regions. It was shown that a slow uniform upstream flow became layered by the action of buoyancy and that at a critical distance $x_c = O(F^{\frac{3}{2}} Ra^{\frac{1}{2}})$ from the sink inertia forces became comparable to the buoyancy and viscous forces. The final region described the convergence of the flow towards the point sink at the origin. This region had a length $O(F^{\frac{1}{2}})$ and the flow there was governed by a pure buoyancy–inertia balance with viscous sublayers providing the transition to the outside flow.

Comparison with laboratory experiments proved to be excellent, but comparison with the only available field data (Wunderlich & Elder 1968) was much less encouraging. The predicted layer thicknesses were considerably smaller than those observed. Two explanations may be suggested for this difference.

First, molecular values of the transport coefficients underestimate the true values and they should thus be replaced by higher eddy coefficients. With the assumption that heat and vorticity diffuse at equal rates, a typical value of the eddy coefficient necessary to coalesce the prototype data onto the theoretical predictions of Imberger (1972) was shown to be $10^{-1}\,\mathrm{cm^2\,s^{-1}}$, a value which compares rather well with the measurements of Orlob & Selna (1970).

Second, the data of Wunderlich & Elder (1968) were collected under normal turbine operating conditions. This meant that the withdrawal rate fluctuated considerably over a 12 h interval and the flow did not have sufficient time to establish itself fully. Recently, Pao & Kao (1974) and Kao, Pao & Wei (1974) considered the start-up of a sink in an infinitely long horizontal duct and illustrated that part of the explanation for the larger observed withdrawal-layer thickness may be the fact that the layer had not reached a steady state and had not fully contracted when the measurements were taken.

However, these and all previous authors assumed that the fluid withdrawn originates from a source at infinity at the level of the sink. This leads to conceptual difficulties which are most obvious if one considers the flow at small Froude number of an inviscid fluid into a line sink.

Upon start-up of a sink in both vertically bounded or unbounded fluid domains the fluid motion set up by the initial pressure field is a potential flow. However, as the motion proceeds the vertical density gradient collapses it into a line jet flowing horizontally into the sink. (See figure 1*a*.) Thus, as demonstrated by Pao & Kao (1974), a steady state is never achieved since this collapse is determined by internal waves moving out from the sink with a finite group velocity. In the unbounded case this difficulty remains even if the fluid is viscous: the radial flow must still change into a layered flow. In a horizontal duct the situation may be remedied by the inclusion of viscosity, which forces the layer to retain the initial uniform motion upstream at all times. This self-consistency of the horizontal-duct problem was assumed by Imberger (1972) and has recently been proved by Pao & Kao (1974).

However, reservoirs have a rear impermeable boundary and laboratory observations of both withdrawal from and discharge of a fluid into a stratified tank by Darden, Imberger & Fischer (1975) suggest that the fluid motion is not modelled by the horizontal-duct configuration, but rather by a deck-of-cards analogy. For, consider a deck of cards resting on a table. If a single card is

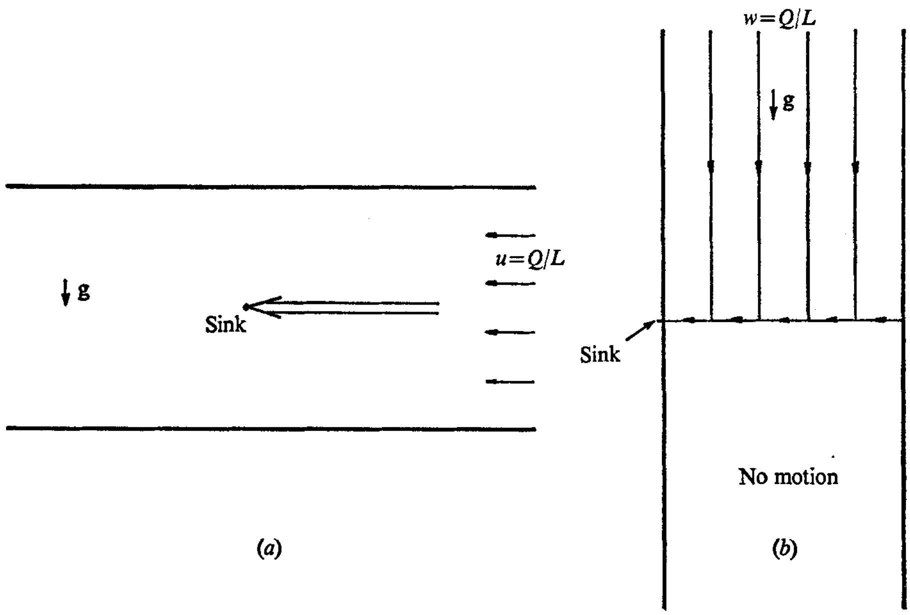

FIGURE 1. (*a*) Flow of an inviscid fluid in a horizontal duct, showing the development of the uniform upstream flow into a withdrawal layer. (*b*) Steady-state solution for an inviscid fluid in a vertical duct moving with a small Froude number.

carefully withdrawn from the centre of the deck that portion of the cards under the selected card remains stationary and the portion above merely falls vertically to take up the space vacated by the withdrawn card. In principle this is exactly what is observed when a fluid is withdrawn from a stratified tank at small Froude numbers.

The above observations suggest the model depicted in figure 1(*b*). The fluid is contained in a vertical duct with the fluid below the sink at rest and that above the sink falling as a solid body. It may be expected that this model will provide a useful description as long as the thickness of the withdrawal layer is small compared with the actual depth of the reservoir or tank. It is shown below that at small Froude numbers the final withdrawal-layer thickness is very much smaller than the reservoir length and the motion above the layer is vertical. Thus, even for reservoirs with small depth-to-length ratios, the withdrawal layer occupies only a small fraction of the depth and the vertical-duct model yields the correct solution. Furthermore, the small Froude number solution for an inviscid fluid approaches a limit which is consistent with the initial boundary condition (see figure 1*b*).

In this paper a solution for the model just described is derived which gives the time development of the flow due to an impulsively started sink with a small Froude number.

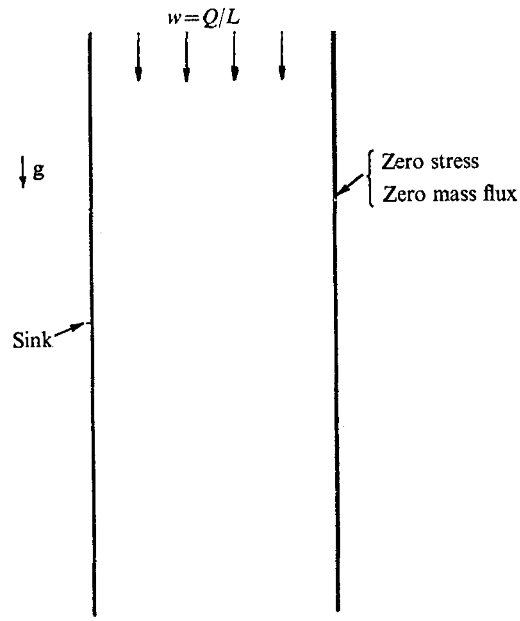

FIGURE 2. The vertical-duct model adopted.

2. Equations governing the flow

The model considered is depicted in figure 2. The sink is situated at the origin of the X, Z co-ordinate system and the water is assumed to be linearly stratified. At the vertical walls the boundary conditions specified are those of zero stress and zero density flux.

The motion which follows a sudden start-up of a discharge Q is characterized by three time scales. These are the period of the internal wave motion, the evolution time of the withdrawal layer and the time required to empty the tank. In this analysis it is assumed that these time scales are ordered and that the evolution time of the withdrawal layer is equal to or larger than the internal wave periods, but much smaller than the time required to empty the tank. With these assumptions it is possible to analyse the flow.

Immediately after the initiation of the motion the flow is pseudo-potential, and thus the correct length scale is L, the width of the strip, and the stream function is $O(Q)$. For the initial development of the motion the time scale T is given by the Brunt–Väisälä period $(\epsilon g)^{-\frac{1}{2}}$, where $\epsilon = -S_0^{-1} dS_1/dZ$, S_0 being the mean density and S_1 the equilibrium stratification. The magnitude S of the density perturbations is $O(S_0 \epsilon L F)$, since it is required that the buoyancy terms balance the unsteady inertia terms at all times.

With these estimates the correct non-dimensional variables to introduce for the initial flow regime are given by

$$x = \frac{X}{L}, \quad z = \frac{L}{Z}, \quad \psi = \frac{\Psi}{Q}, \quad s = \frac{S}{S_0 \epsilon L F}, \quad t = T(\epsilon g)^{\frac{1}{2}}.$$

In terms of these variables the Boussinesq approximation to the equations of motion becomes

$$\nabla^2\psi_t + F(\psi_z \nabla^2\psi_x \nabla^2\psi_z) = s_x + (Pr/Ra)^{\frac{1}{2}}(\nabla^2\psi_{zz} + \nabla^2\psi_{xx}), \tag{1}$$

$$s_t + \psi_x + F(-\psi_x s_z + \psi_z s_x) = (Pr\,Ra)^{-\frac{1}{2}}(s_{xx} + s_{zz}), \tag{2}$$

where $F = Q/L^2(\epsilon g)^{\frac{1}{2}}$, $Ra = g\epsilon L^4/\nu D$, $Pr = \nu/D$, ν is the kinematic viscosity and D is the coefficient of salt or heat diffusion.

The approximation sought is obtained by setting $F = 0$ and $Ra = \infty$; this yields the flow equations for an inviscid non-diffusive fluid moving with a small Froude number:

$$\nabla^2\psi_t = s_x, \quad s_t + \psi_x = 0. \tag{3), (4}$$

In both model tank experiments and prototype flows the Rayleigh number Ra is always very large. The meaning of the small Froude number assumption becomes clear by noting that the Froude number may be written as

$$F = \frac{(\epsilon g)^{-\frac{1}{2}}}{L^2/Q} = \frac{\text{wave period}}{\text{time taken for the fluid to fall a distance } L}.$$

Thus the assumption $F = 0$ is valid provided that the flow evolves into a layer before the linear density stratification has been appreciably modified by the vertical convection of the density perturbation. In other words the change in density gradient induced by the falling mass of fluid above the sink level is ignored.

If F is small but not infinitesimal then the steady-state solution found here will be an outer solution in the spirit of Imberger (1972). Furthermore, for flow in a reservoir of depth-to-length ratio λ it should be noted that the convective acceleration terms are now $O(\lambda^{-1}F)$. For the given solution to be uniformly valid in time for such a case it is required that $\lambda^{-1}F$ also is small.

The solution to (3) and (4) will be given in § 3. However, as discussed in the introduction, this initial flow changes from a potential flow to a flow with a thin withdrawal layer at the origin. Thus as time proceeds the vertical scale changes from L to δ, the withdrawal-layer thickness, and the solutions to (3) and (4) cannot be expected to hold for large times. Both the vertical length scale and the time scale of the motion change as the motion proceeds in such a way that the balance of forces adjusts until the viscous forces are of the same magnitude as the buoyancy and unsteady inertia forces.

When this triple force balance has been achieved the time scale has become $O(Ra^{\frac{1}{6}}/(\epsilon g)^{\frac{1}{2}})$, and vertical length scale δ/L has reduced to $O(Ra^{-\frac{1}{6}})$ and the density perturbation has become $O(S_0 \epsilon LF\,Ra^{\frac{1}{6}})$. With this scaling the convective inertia terms become $O(F\,Ra^{\frac{1}{3}})$ and as in the horizontal-duct problem investigated by Imberger (1972) may be neglected provided that the critical distance x_c, equal to $LF^{\frac{3}{2}}Ra$, is small compared with the duct width L.

It is therefore necessary to rescale the previous non-dimensional variables and introduce the following new variables:

$$\xi = x, \quad \eta = z\,Ra^{\frac{1}{6}}, \quad \tau = t\,Ra^{-\frac{1}{6}}, \quad \rho = s\,Ra^{-\frac{1}{6}}.$$

Equations (1) and (2) then become

$$Ra^{-\frac{1}{3}}\psi_{\xi\xi\tau}+\psi_{\eta\eta\tau}+O(F\,Ra^{\frac{1}{3}}) = \rho_{\xi}+Pr^{\frac{1}{2}}\psi_{\eta\eta\eta\eta}+O(Pr^{\frac{1}{2}}Ra^{-\frac{1}{3}}) \tag{5}$$

and
$$\rho_{\tau}+\psi_{\xi}+O(F\,Ra^{\frac{1}{3}}) = Pr^{\frac{1}{2}}\rho_{\eta\eta}+O(Pr^{-\frac{1}{2}}Ra^{-\frac{1}{3}}), \tag{6}$$

where the term $\psi_{\xi\xi\tau}$ has been retained so that the solutions of (3) and (4), governing the small time behaviour, will automatically match the solutions of (5) and (6).

Elimination of the density ρ from (5) and (6) yields

$$\psi_{\eta^{(6)}}-(1+Pr)\,Pr^{-\frac{1}{2}}\psi_{\eta^{(4)}\tau}+Ra^{-\frac{1}{3}}\psi_{\xi\xi\tau\tau}+\psi_{\eta\eta\tau\tau}+\psi_{\xi\xi} = 0, \tag{7}$$

where once again terms $O(Ra^{-\frac{1}{3}})$ have been neglected except for the single term $\psi_{\xi\xi\tau\tau}$, which must be retained to preserve the uniform validity of the approximation.

3. Solutions for small times: inviscid flow

The equation for ψ valid for small times is obtained by eliminating ρ from (3) and (4), namely

$$\nabla^2\psi_{tt}+\psi_{xx} = 0. \tag{8}$$

This equation must now be solved subject to the following boundary conditions:

$$\psi(0,z,t) = -\tfrac{1}{2}\,\mathrm{sgn}\,(z)\,H(t), \quad \psi(1,z,t) = \tfrac{1}{2}H(t), \tag{9), (10}$$

$$\psi(x,\infty,t) = (x-\tfrac{1}{2})\,H(t), \quad \psi(x,-\infty,t) = \tfrac{1}{2}H(t). \tag{11), (12}$$

Equation (8) is most easily solved by taking a Laplace transform in t and then a Fourier transform in z. These are defined as follows:

$$\overline{\psi}(x,z,s) = \int_0^\infty \psi(x,z,t)\,e^{-st}\,dt \tag{13}$$

and
$$\overline{\overline{\psi}}(x,k,s) = \frac{1}{(2\pi)^{\frac{1}{2}}}\int_{-\infty}^{\infty}\overline{\psi}(x,z,s)\,e^{ikz}\,dz. \tag{14}$$

With this convention (8)–(10) yield

$$\overline{\overline{\psi}}_{xx}-\alpha^2\overline{\overline{\psi}} = 0, \tag{15}$$

where
$$\alpha^2 = s^2k^2/(s^2+1), \tag{16}$$

$$\overline{\overline{\psi}}(0,k,s) = -\frac{i}{2sk}\left(\frac{2}{\pi}\right)^{\frac{1}{2}}, \quad \psi(1,k,s) = \left(\frac{\pi}{2}\right)^{\frac{1}{2}}\frac{1}{s}\,\delta(k). \tag{17), (18}$$

The solution to (15) satisfying (17) and (18) is given by

$$\begin{aligned}\overline{\overline{\psi}} &= \left(\frac{\pi}{2}\right)^{\frac{1}{2}}\frac{1}{s}\,\delta(k)\frac{\sinh\alpha x}{\sinh\alpha}-\frac{i}{(2\pi)^{\frac{1}{2}}}\frac{1}{sk}\frac{\sinh\alpha(1-x)}{\sinh\alpha} \\ &= \overline{\overline{\psi}}_1+\overline{\overline{\psi}}_2,\end{aligned} \tag{19}$$

where
$$\overline{\overline{\psi}}_1 = \left(\frac{\pi}{2}\right)^{\frac{1}{2}}\frac{1}{s}\,\delta(k)\frac{\sinh\alpha x}{\sinh\alpha} \tag{20}$$

and
$$\overline{\overline{\psi}}_2 = \frac{-i}{(2\pi)^{\frac{1}{2}}}\frac{1}{sk}\frac{\sinh\alpha(1-x)}{\sinh\alpha}. \tag{21}$$

The inversion of $\bar{\bar{\psi}}_1$ is straightforward and leads to the contribution

$$\psi_1(x,z,t) = \tfrac{1}{2}xH(t). \tag{22}$$

The inversion of $\bar{\bar{\psi}}_2$ is more complicated, but may be carried out by the method of residues:

$$\psi_2(x,z,t) = \frac{-i}{(2\pi)^{\frac{1}{2}}}\frac{1}{(2\pi)^{\frac{1}{2}}}\int_{-\infty}^{-\infty}\frac{1}{2\pi i}\int_{\gamma-i\infty}^{\gamma+i\infty}\frac{1}{sk}\frac{\sinh[\alpha(1-x)]\,e^{-ikz+st}dk\,ds}{\sinh\alpha}, \tag{23}$$

where γ is chosen such that all the residues lie to the left of the path of integration.

Consider first the Fourier inverse

$$\bar{\psi}_2(x,z,s) = \frac{-i}{2\pi s}\int_{-\infty}^{\infty}\frac{1}{k}\frac{\sinh[\alpha(1-x)]\,e^{-ikz}dk}{\sinh\alpha}. \tag{24}$$

The only singularities of the integrand are simple poles and these are located at

$$k_n = \pm in\pi(s^2+1)^{\frac{1}{2}}/s \quad (n = 0, 1, \ldots), \tag{25}$$

which all lie on the imaginary axis provided that $\mathrm{Re}(s)$ is chosen large enough. The theory of residues leads to the solution for $\bar{\psi}_2$ for $z > 0$:

$$\bar{\psi}_2(x,z,s) = -\frac{(1-x)\,\mathrm{sgn}\,z}{2}\frac{}{s} - \sum_{n=1}^{\infty}\frac{(-1)^n}{\pi}\frac{\sin[n\pi(1-x)]}{n}\frac{1}{s}\exp\left[\frac{-n\pi(s^2+1)z^{\frac{1}{2}}}{s}\right]. \tag{26}$$

Carrying out the Laplace inverse and combining this with (22) leads to the solution for ψ for $z > 0$:

$$\psi(x,z,t) = (x-\tfrac{1}{2})H(t) + \sum_{n=1}^{\infty}\frac{(-1)^n}{\pi}\frac{\sin n\pi(1-x)}{n}\left\{J_0\left[2\left(\frac{t}{n\pi z}\right)^{\frac{1}{2}}\right]\right\}$$
$$\times\left[1-\frac{1}{n\pi z}\int_0^{\infty}\frac{J_1\{(u^2-n^{-2}\pi^{-2}z^{-2})^{\frac{1}{2}}\}\,du}{[u^2-(1/n^2\pi^2z^2)]^{\frac{1}{2}}}\right]. \tag{27}$$

Similarly, for $z < 0$ the solution is given by

$$\psi(x,z,t) = \tfrac{1}{2}H(t) - \sum_{n=1}^{\infty}\frac{(-1)^n}{\pi}\frac{\sin n\pi(1-x)}{n}\left\{J_0\left[2\left(-\frac{t}{n\pi z}\right)^{\frac{1}{2}}\right]\right\}$$
$$\times\left[1+\frac{1}{n\pi z}\int_0^{\infty}\frac{J_1\{(u^2-1/n^2\pi^2z^2)^{\frac{1}{2}}\}}{(u^2-1/n^2\pi^2z^2)^{\frac{1}{2}}}\,du\right]. \tag{28}$$

As already mentioned in the introduction, Pao & Kao (1974) showed that a horizontal duct acts as a wave guide and the internal waves emanating from the sink travel upstream unattenuated. The situation here is quite different because of the presence of the vertical walls. The curving of the streamlines produces baroclinic vorticity which may be decomposed into left- and right-going waves with phases such that they will always add destructively, so that the disturbance initiated at the sink dies out exponentially in both the upward and downward directions. This is most clearly illustrated if we look at the large time behaviour of the solution given by (26). Approximating α by its value at $s = 0$ and inverting the Laplace transform first yields an expression for the Fourier transform of $\psi_2(x,z,t)$:

$$\phi_2(x,k,t) \sim \int_0^t\sum_{n=0}^{\infty}[H\{t'+k(1-x)-(2n+1)k\}-H\{(t'-k(1-x)-(2n+1)k\}]\,dt'. \tag{29}$$

The integrand in (29) exhibits two series of wavelike motions, one travelling to the right and the other to the left with speed $(\epsilon g)^{\frac{1}{2}}/k$. Their combined effect, however, cancels and (29) reduces to a form independent of time:

$$\phi_2(x, k, t) \sim -2k(1-x).$$

This is quite different from the behaviour in a horizontal duct, where only outgoing waves exist and these propagate unattenuated except for viscous damping.

4. Solutions for large times: steady viscous flow

For times larger than $O((\epsilon g)^{\frac{1}{2}} Ra^{\frac{1}{6}})$ but smaller than $O(L^2/Q)$ a quasi-steady state exists and the fluid motion is adequately described by the steady counterpart to (7), namely

$$\psi_{\eta^{(6)}} + \psi_{\xi\xi} = 0. \tag{30}$$

The boundary conditions (9)–(12) must be supplemented by zero-stress and zero-mass-flux conditions at the wall. The Fourier transform of ψ with respect to the vertical co-ordinate η which satisfies the boundary conditions is given by

$$\phi(\xi, k) = \left(\frac{\pi}{2}\right)^{\frac{1}{2}} \xi\delta(k) - \frac{i}{(2\pi)^{\frac{1}{2}}} \frac{1}{k} \frac{\sinh[k^3(1-\xi)]}{\sinh k^3}. \tag{31}$$

The only singularities, apart from the $\delta(k)$ at the origin, are simple poles which are located at

$$k_n = (n\pi)^{\frac{1}{3}}\{e^{\frac{1}{6}i\pi}, e^{\frac{1}{2}i\pi}, e^{\frac{5}{6}i\pi}, e^{\frac{7}{6}i\pi}, e^{\frac{3}{2}i\pi}, e^{\frac{11}{6}i\pi}\}. \tag{32}$$

Hence the inverse of (31) may be obtained simply by the theory of residues. For $\eta > 0$

$$\begin{aligned}\psi(\xi, \eta) = {} & (\xi - \tfrac{1}{2}) - \frac{1}{3} \sum_{n=1}^{\infty} (-1)^n \frac{\sin[n\pi(1-\xi)] \exp[-(n\pi)^{\frac{1}{3}}\eta]}{n\pi} \\ & - \frac{2}{3} \sum_{n=1}^{\infty} (-1)^n \frac{\sin[n\pi(1-\xi)]}{n\pi} \cos\left[\frac{3^{\frac{1}{2}}}{2}(n\pi)^{\frac{1}{3}}\eta\right] \exp\left[-\frac{(n\pi)^{\frac{1}{3}}\eta}{2}\right]\end{aligned} \tag{33}$$

and for $\eta < 0$

$$\begin{aligned}\psi(\xi, \eta) = {} & \tfrac{1}{2} + \frac{1}{3} \sum_{n=1}^{\infty} (-1)^n \frac{\sin[n\pi(1-\xi)]}{n\pi} \exp[(n\pi)^{\frac{1}{3}}\eta] \\ & + \frac{2}{3} \sum_{n=1}^{\infty} (-1)^n \frac{\sin[n\pi(1-\xi)]}{n\pi} \exp\left[\frac{(n\pi)^{\frac{1}{3}}\eta}{2}\right] \cos\left[\frac{3^{\frac{1}{2}}}{2}(n\pi)^{\frac{1}{3}}\eta\right].\end{aligned} \tag{34}$$

5. A solution uniformly valid in time

In principle the solution of (7) may be obtained in the same way as in the two previous cases. The transform variable $\bar{\bar{\psi}}$ which satisfies the boundary conditions (9)–(12) and yields zero stress at the walls and zero mass flux across the walls is again given by (19), but with the function α now given by

$$\alpha^2 = \frac{k^4 + (1+Pr)\, Pr^{-\frac{1}{2}} sk^2 + s^2}{Ra^{-\frac{1}{3}} s^2 + 1}. \tag{35}$$

Using the notation of the previous section,

$$\psi = \psi_1 - \frac{1}{4\pi^2}\int_{\gamma-i\infty}^{\gamma+i\infty}\int_{-\infty}^{\infty}\frac{1}{ks}\frac{\sinh[\alpha(1-\xi)]\,e^{s\tau-ik\eta}\,dk\,ds}{\sinh\alpha}. \tag{36}$$

The integrand in (36) is an odd function of k and ψ may therefore be written in the form

$$\psi = -\frac{i}{\pi}\int_0^{\infty}\frac{F(\xi,k,\tau)\sin k\eta}{k}\,dk+\psi_1, \tag{37}$$

where
$$F(\xi,k,\tau) = \frac{1}{2\pi i}\int_{\gamma-i\infty}^{\gamma+i\infty}\frac{1}{s}\frac{\sinh\alpha(1-\xi)}{\sinh\alpha}\,e^{st}\,ds. \tag{38}$$

The path of integration in (38) is parallel to the complex s axis and to the right of all singularities. There are no branch points; the only contributions to the integral in (38) come from a pole at $s = 0$ (the steady solution ψ_2 derived in the previous section) and from poles where

$$\alpha^2 = -n^2\pi^2,$$

or equivalently at points in the s plane given by

$$s_n^{(1,2)} = \frac{-(1+Pr)\,k^4 \pm \{(1+Pr)^2k^8 - 4Pr(k^2+n^2\pi^2Ra^{-\frac{1}{3}})(k^6+n^2\pi^2)\}^{\frac{1}{2}}}{2(k^2+n^2\pi^2Ra^{-\frac{1}{3}})\,Pr^{\frac{1}{2}}}. \tag{39}$$

Thus we may further subdivide the contribution from the first part of (37) into a steady part ψ_2 and a time-dependent part ψ_3. The value of ψ_2 is given by (33) and (34). The contribution ψ_3 may be evaluated by noting that, for real $k > 0$, the real parts of $s_n^{(1)}$ and $s_n^{(2)}$ are less than or equal to zero for every n, so that the solution ψ_3 will be wavelike and will decay exponentially with time. Thus the integral in (38) may be evaluated by summing the residues at the poles. After some tedious algebra ψ_3 may be shown to be given by

$$\psi_3(\xi,\eta,\tau) = \frac{2}{\pi}\sum_{n=1}^{\infty}(-1)^n\frac{\sin n\pi(1-\xi)}{n\pi}\,E_n(\eta,\tau), \tag{40}$$

where

$$E_n(\eta,\tau) = \int_0^{\infty}\frac{(k^2+1)\,[r_n^{(2)}\exp(ar_n^{(1)}\tau)\,(b+r_n^{(1)2}) - r_n^{(1)}\exp(ar_n^{(2)}\tau)\,(b+r_n^{(2)2})]}{k(ck^6+b)\,[k^8-4(1+k^2)\,(ck^6+b)]^{\frac{1}{2}}}$$
$$\times\sin(Ra^{-\frac{1}{6}}n\pi\eta k)\,dk, \tag{41}$$

with
$$r_n^{(1,2)} = \frac{-k^4 \pm [k^8-4(1+k^2)\,(ck^6+b)]^{\frac{1}{2}}}{2(1+k^2)}, \tag{42}$$

$$a = \left(\frac{1+Pr}{Pr^{\frac{1}{2}}}\right)n^2\pi^2Ra^{-\frac{1}{3}}, \quad b = \frac{Pr\,Ra}{(1+Pr)^2n^4\pi^4}, \tag{43), (44}$$

and
$$c = Pr/(1+Pr)^2. \tag{45}$$

The complete solution for the stream function is thus

$$\psi(\xi,\eta,\tau) = \psi_1+\psi_2+\psi_3. \tag{46}$$

The evaluation of $E_n(\eta,\tau)$ was carried out numerically by Filon's method.

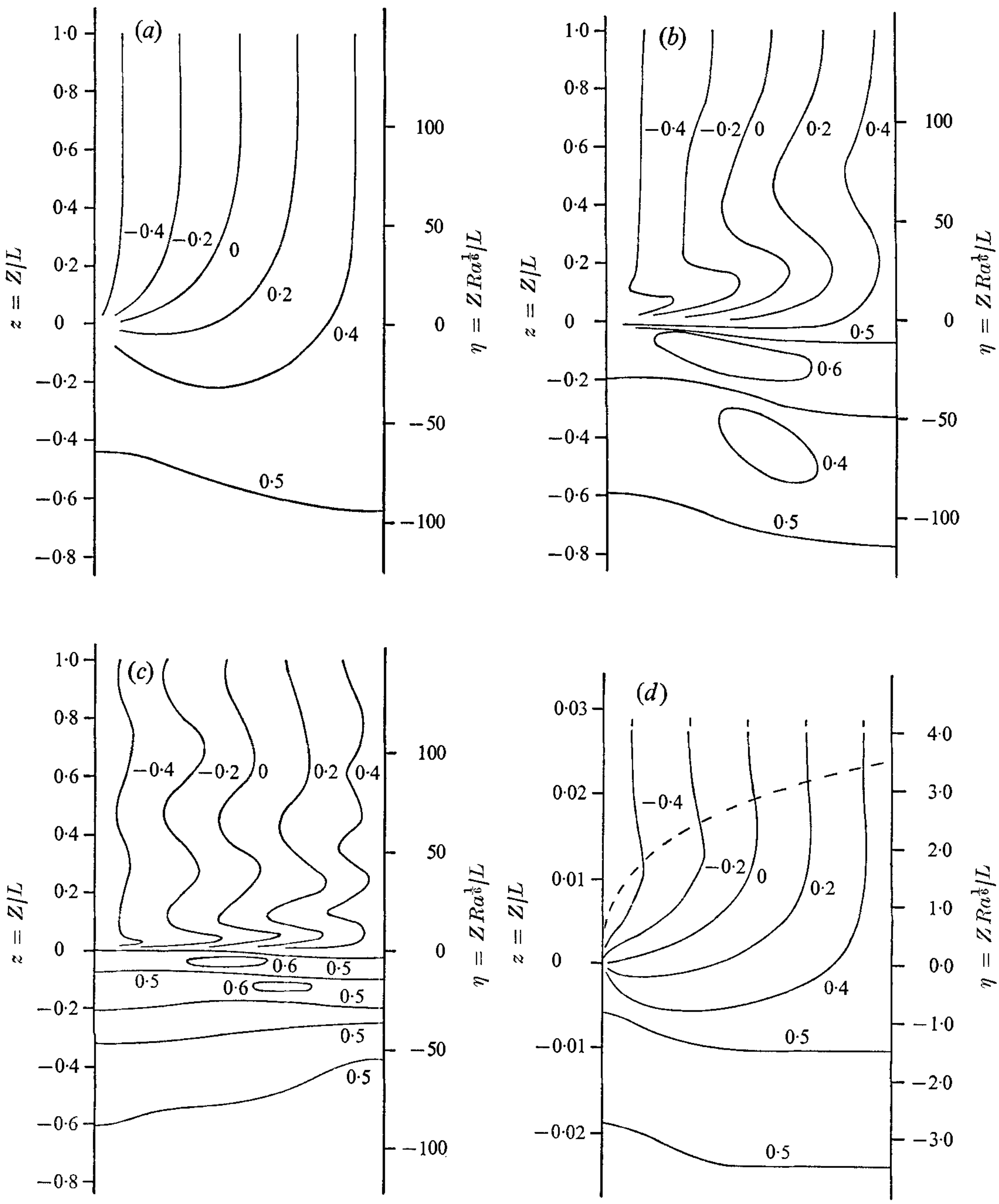

FIGURE 3. Streamlines as functions of time. $Pr = 10^3$, $Ra = 10^{13}$, $t = T(\epsilon g)^{\frac{1}{2}}$, $\tau = T(\epsilon g)^{\frac{1}{2}} Ra^{-\frac{1}{6}}$. (a) $t = 1$, $\tau = 0{\cdot}022$. (b) $t = 6$, $\tau = 0{\cdot}129$. (c) $t = 20$, $\tau = 0{\cdot}43$. (d) $t = \infty$, $\tau = \infty$. – – –, line of zero horizontal velocity as predicted by, for example, (47).

6. Discussion

The solutions derived here are applicable when the Froude number F, the inverse Ra^{-1} of the Rayleigh number, the inverse Re^{-1} of the Reynolds number and the product $F Ra^{\frac{1}{3}}$ are all much less than one. The Prandtl number is assumed to be $O(1)$. The development with time of the stream function is shown in figures 3(a)–(d) for salt-stratified water and a Rayleigh number typical of a laboratory situation. However, the values of the Rayleigh and Prandtl numbers will only influence the presentation of the solution at intermediate times (figures 3b, c), since for both times smaller than $O(\epsilon g)^{-\frac{1}{2}}$ and larger than $O(Ra^{\frac{1}{3}}(\epsilon g)^{-\frac{1}{2}})$ the scaling incorporates the dependence on both Ra and Pr. Thus the representations shown in figures 3(a) and (d) are valid for all values of the Rayleigh and Prandtl numbers.

Inspection of figures 3(a)–(c) shows that the predicted flow development may be expected to yield a realistic description of the motion in a tank with a free surface provided that the depth-to-length ratio is greater than one. However, the steady-state solution shown in figure 3(d) will represent the flow in a shallow tank which has a depth-to-length ratio greater only than $O(Ra^{-\frac{1}{6}})$.

The asymptotic limit adopted here is identical to that used by Imberger (1972) and thus it is not surprising that, as η and ξ tend to zero, the steady-state solution given by (33) and (34) approaches

$$\psi(\zeta) = \int_0^\infty \frac{e^{-p^3}}{p} \sin p\zeta \, dp, \tag{47}$$

where $\zeta = \eta/\xi^{\frac{1}{3}}$. This is the same limit as in the horizontal-duct problem. Hence the inner solution found by Imberger (1972) is also valid here and once again we have a partitioning of the flow into three distinct regions, each characterized by a different force balance.

This asymptotic behaviour explains why some previous investigators found good correlation between experimental data, taken mostly close to the sink, and theories established for either an unbounded fluid or one contained in a horizontal duct. As may be seen in figure 3(d), the layer thicknesses, defined by the point of zero horizontal velocity, agree quite well out to a distance of about one-fifth of the length of the tank. Beyond this the present solution predicts a somewhat thinner withdrawal layer.

In most experimental situations the depth-to-length ratio is smaller than one, but considerably larger than $Ra^{-\frac{1}{6}}$. Kao *et al.* (1974) have recently shown that in such cases the initial flow resembles potential flow in a horizontal duct, the upstream velocity being uniform and horizontal. This is made possible by the falling free surface, which induces a horizontal velocity equal to $Q/d(1-\xi)$, where d is the depth. They further showed that this uniform flow is modified initially only by outgoing waves. This is not a contradiction of the above work, but rather a natural consequence of the small depth-to-length ratio. Since the fluid can move horizontally, without violating any boundary condition, no internal vorticity is generated upstream of where the outgoing waves have penetrated and hence no left-moving internal waves are generated.

However, as the motion proceeds, and the first waves have passed, the horizontal motion will be progressively replaced by a vertical motion which in turn will lead to the production of internal vorticity which may be decomposed into internal right- and left-going waves. The flow will then be described by the vertical-duct model and a pseudo-steady state will be reached after times $O(Ra^{\frac{1}{3}}/(\epsilon g)^{\frac{1}{2}})$.

This explanation is further reinforced if one analyses the scaling of the horizontal-duct problem in a similar fashion to that described in §2 above. The appropriate vertical scale now becomes the depth d since the equations must describe the transition from a uniform flow, extending over the whole duct depth, to a withdrawal layer at the origin, of thickness $O(Ra^{-\frac{1}{6}}d)$, where the Rayleigh number is now based on the depth d. The correct horizontal length scale is $Ra^{\frac{1}{3}}d$ and the time scale becomes $Ra^{\frac{1}{2}}/(\epsilon g)^{\frac{1}{2}}$. The equation for the stream function then becomes identical to (7), whose steady form has been solved by Imberger (1972) and whose inviscid limit has been obtained by Pao & Kao (1974). However, the much larger time and length scales must be emphasized, since these make it difficult to achieve a horizontal-duct flow in the laboratory, unless the depth is very small.

Lastly, it is interesting to apply the above results to the field data obtained by Wunderlich & Elder (1968) in the T.V.A. reservoirs. The field data from the Fontana reservoir suggest a typical depth of 60 m, a Väisälä frequency of $0{\cdot}02\ \mathrm{s}^{-1}$, a length of 30 km and a Froude number, based on the length, equal to 10^{-8}. In accordance with the work of Orlob & Selna (1970), a typical value for the kinematic viscosity and diffusivity of heat is $10^{-5}\ \mathrm{m}^2\,\mathrm{s}^{-1}$. This leads to a value of Ra of 10^{24}, which in turn means that the time taken to reach a fully steady flow is close to 3 days. This must be interpreted with care as $FRa^{\frac{1}{3}}$ is $O(1)$, but there is no doubt that the flow had not reached a steady state when the data were taken.

REFERENCES

Darden, B., Imberger, J. & Fischer, H. B. 1975 *J. Hyd. Div., Proc. A.S.C.E.* (in Press).

Imberger, J. 1972 *J. Fluid Mech.* **53**, 171–181.

Kao, T. W. 1965 *J. Fluid Mech.* **21**, 535–543.

Kao, T. W. 1970 *Phys. Fluids*, **13**, 558–564.

Kao, T. W., Pao, H. P. & Wei, S. N. 1974 *J. Fluid Mech.* **56**, 689–710.

Koh, R. C. Y. 1966 *J. Fluid Mech.* **24**, 555–575.

Orlob, G. T. & Selna, L. G. 1970 *J. Hyd. Div., Proc. A.S.C.E.* **96** (HY2), 391–410.

Pao, H. P. & Kao, W. T. 1974 *J. Fluid Mech.* **65**, 657–688.

Wunderlich, W. O. & Elder, R. A. 1968 *A.S.C.E. Specialty Conf. on Current Res. into Effects of Reservoirs on Water Quality, Portland, Oregon.*

Yih, C. S. 1965 *Dynamics of Nonhomogeneous Fluids.* Macmillan.